Jurnal Polimesin
Department of Mechanical Engineering
State Polytechnic of Lhokseumawe
http://e-jurnal.pnl.ac.id/polimesin
e-ISSN : 2549-1999 No. : 6 Month : December
p-ISSN : 1693-5462 Volume : 22 Year : 2024

Article Processing Dates: Received on 2024-10-04, Reviewed on 2024-10-12, Revised on 2024-11-02, Accepted on 2024-11-04 and Available online on 2024-12-30

Modeling the effect of bullet velocity and composite fiber orientation on the ballistic impact strength of E-glass/isophthalic polyester composites

FRZ Fahmi[1,*], H Hermawan[2], FD Hanggara[1]
[1]Mechanical Engineering, UIN Maulana Malik Ibrahim, Malang, 65144, Indonesia
[2]Civil and Construction Engineering, National Taiwan University of Science and Technology, Taipei 106, Taiwan
*Corresponding author: farizrifqizf@uin-malang.ac.id

Abstract

Numerical simulation has been widely used as a cost-effective and practical solution to understand phenomena previously determined only through experiment. One example is ballistic impact simulation using the finite element method. The simulation of ballistic impact was used to determine the effect of fiber orientation and bullet velocity on the ballistic impact strength of E-glass/isophthalic polyester. The analysis and simulation process were conducted using ANSYS Workbench v19.2 software. The simulation involved firing a 9 mm FMJ Parabellum bullet with a mass of 6.98 grams at a composite panel measuring 100×100×0.57 mm with 12 layers at specified velocities. This study varied fiber orientation ([±45°] and [0°, 90°]) and bullet velocities (300, 500, and 800 m/s), using symmetrical laminate arrangements. The simulation results showed that the E-glass/isophthalic polyester composite with a fiber orientation of [±45°] has 16.51% higher ballistic strength compared to the [0°, 90°] fiber orientation. The highest ballistic impact strength for the [±45°] fiber orientation occured at 500 m/s, surpassing the 300 m/s and 800 m/s velocities by 12.92% and 43.81%, respectively. The Wen model was used for the validation process, and the error values between the computed and modeling results for the E-glass/isophthalic polyester composite ranged between 1.62% and 20.64%.

Keywords:
Isophthalic polyester, E-glass, composite laminate, explicit dynamic, ballistic impact.

1 Introduction

Synthetic fiber-reinforced polymer composites have been extensively researched over the past century. These composites increasingly replace conventional structural materials like wood, metal, and reinforced concrete [1]. Amongst newly-developed composites, Fiber Reinforced Polymers (FRP) are renowned for their superior mechanical properties. Polymer composites with fillers typically exhibit enhanced thermal, physical, electrical, and mechanical properties due to efficient filling, processing, and curing [2], [3]. These materials demonstrate high strength and stiffness ratios. FRP is often used in manufacturing bulletproof products. For ballistic impact protection, high-performance fibers, such as glass, aramid, and carbon fiber, are commonly utilized [4].

As a matrix of FRP composite, polyester/polyethylene terephthalate is a high-performance, low-cost thermosetting polymer that is commonly used in packaging materials due to its hardness, abrasion resistance, solvent resistance, electrical insulation properties, and excellent rigidity [5], [6], [7]. Glass fibers are the most commonly used reinforcement for advanced composite materials across various applications [8]. Although glass fibers have a relatively low density and high strength, their Young's modulus could be higher. This results in a high strength-to-weight ratio but only with a moderate modulus-to-weight ratio. Despite this drawback, glass fibers remain widely used for reinforcing polyester called Glass Fibre Reinforced Plastic (GFRP) [9].

Composite armors comprise multiple layers of FRP composite materials, typically including metals, composites, ceramics, and other tightly bonded substances. This type of armor has led to significant innovations in the industry. Despite achieving several notable milestones, the ongoing progress in ballistic technology demands the development of armor systems with superior mechanical and impact performance, reduced weight, improved formability, and the ability to withstand high-level threats [10].

Numerous experimental ballistics tests have been conducted to investigate the mechanical responses of woven composites under ballistic impact. The finite element method and analytical modeling are the most commonly used numerical techniques within the community for simulating mechanical responses under ballistic impact [11].

The ballistic performance of FRP composites under impact is largely determined by a combination of internal and external factors, making it challenging to accurately predict their ballistic limits. In recent years, researchers have dedicated efforts to develop accurate analytical and numerical methods to forecast these limits. Additionally, they have sought to improve their understanding of how various factors affect the high-speed impact behavior of FRP composites. A comprehensive review of the theoretical and numerical research can be found in [12], serving as a guide for modeling ballistic limits and designing bulletproof composites.

The primary features of impact and penetration issues include high-intensity loading and short-duration forces. Significant stress is concentrated in the contact zone between the projectile and target during the impact and penetration phases, causing plastic deformation and target failure. The ballistic behavior of Fiber Reinforce Plastic (FRP) composites under ballistic impact largely depends on the simultaneous interaction of internal and external factors, as illustrated in Fig. 1 [12].

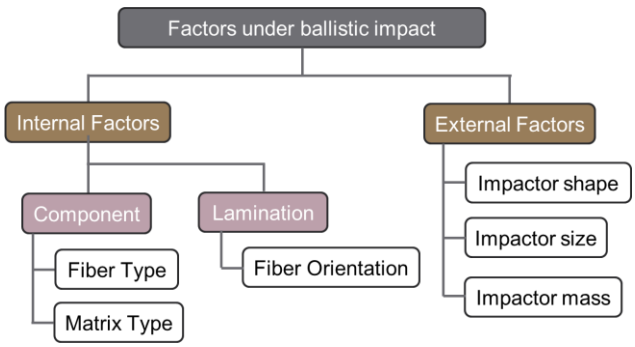

Fig. 1. Factors affecting the ballistic limit of FRP composite.

Elamvazhudi and Boodala [13] investigated the ballistic impact by varying fiber orientations. Their findings revealed that the damage mode was influenced by factors such as the projectile, initial velocity, mass, and height of the impactor. The fiber orientation, laminate thickness, fiber type, and fiber stacking sequence were the primary factors affecting ballistic resistance. Additionally, the arrangement of fibers, including their orientation, significantly affected the enhancement of the laminate's tensile strength. Mahesh et al. [14] studied the impact of thickness and projectile shape on composites at a velocity of 300 m/s. The study found that the ogival-shaped projectiles caused the most severe damage, resulting in a deeper penetration into the

flexible composite blocks, followed by hemispherical and flat-shaped projectiles.

An analysis was performed to evaluate the effect of fiber orientation on the ballistic impact strength of the E-glass/isophthalic polyester composite. The study specifically examined and compared different fiber orientations and the number of layers within the composite material. The ANSYS Mechanical APDL R15.0 software was employed to analyze the propagation of failures. Numerical simulations, like experimental studies based on theoretical research, are efficient but may not fully capture real-world conditions [15], [16]. However, through computer implementation, accurate simulation models can reveal the principles of penetration and the dynamic response of the target.

Karthick and Ramajeyathilagam also studied ballistic speed limits [17]. In their study, the composite consisted of eight layers, and a cylindrical steel projectile with a shank diameter of 6.36 mm, a length of 25.3 mm, and a mass of 6.42 g was used to impact GFRP and CFRP armors at a velocity of 110 m/s. The reported ballistic speed limit ranged between 52.8 m/s and 63.7 m/s.

Wen [18] developed a calculation model to predict ballistic speed limits. This model assumed that the average pressure applied normally to the projectile surface can be divided into two components: cohesive resistive pressure from the quasi-static elastic-plastic deformation of the composite and dynamic resistive pressure from the impact velocity.

Wen discussed the resistive pressure during ballistic impact and provided the assumption that the initial pressure σ is applied to the surface of the projectile, and the rejection of penetration and the perforation projectile by the laminate is divided into two parts: cohesive quasi-static resistive pressure and dynamic resistive pressure. Wen's ballistic model formula is presented in Eq. 1.

$$V_b = \frac{3\pi\sqrt{\rho_t \sigma_e} D^2 T}{8G}\left[1 + \sqrt{1 + \frac{32G}{9\pi\rho_t D^2 T}}\right] \quad (1)$$

where V_b is the ballistic speed limit (m/s), β is the dimensional constant, σ_e is the equivalent stress (MPa), ρ_t is the density of the composite (kg/m^3), D is the projectile diameter (mm), T is the composite thickness (mm), and G is the mass of the projectile (g).

This study investigates the effect of bullet velocity and fiber orientation in composite materials on the impact strength of E-glass/isophthalic polyester composites. Various bullet velocities were employed on a 12-layer composite with different fiber orientation directions.

2 Research Materials and Methods

The investigation supported by ANSYS Mechanical APDL R15.0 provides robust and powerful results of finite element analysis. The opted material as a bulletproof composite was an isopthalic-polyester matrix with E-glass fiber reinforcement. The fiber and matrix were mixed by the ratio of 1:1.7 by fraction volume. E-glass/isophthalic-polyester composites were built in laminar form with 100×100×0.57 mm, consisting of 8, 12 and 16 layers. E-glass fiber reinforcement varied in [0°,90°] and [±45°] orientation. Brass projectile with a caliber 9 mm has a mass of 6.98 grams which is modeled according to NIJ-0101.04 [19]. The type of element used in the ANSYS software was a solid tetrahedral, as shown in Fig. 2.

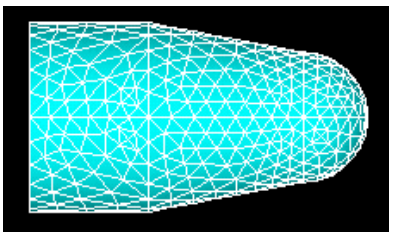

Fig. 2. Tetrahedral projectile element.

The composite material used was type E glass fiber (E-glass) as reinforcing fiber and isophthalic-polyester as the matrix, with a reinforcing fiber volume fraction of 36.51%. Mechanical property data was obtained based on ASM Handbook volume 21 [20] (Table 1).

Table 1. Mechanical properties of E-glass/isophthalic-polyester composite

Mechanical properties	DCMU Unidirectional
Young modulus longitudinal (GPa)	25.80
Young modulus transversal (GPa)	8.0
Young modulus z axis (GPA)	8.0
Poisson ratio (yx-axis)	0.09
Poisson ratio (zx-axis)	0.09
Poisson ratio (zy-axis)	0.29
Shear modulus in the xy-axis (GPa)	8.40
Shear modulus in the yx-axis (GPa)	3.10
Shear modulus in the xy-axis (GPa)	8.40
Density (kg/m^3)	1680

The material used for the projectile was brass with mechanical properties based on past research by Zochowski [21] and Gmitrzuk [22] (Table 2).

Table 2. Mechanical properties of projectile

Density (kg/m^3)	11340
Young modulus x axis (GPa)	16×10^9
Poisson ratio xy axis	0.44

The applied velocities of the bullet analyzed using ANSYS were 300, 500, and 800 m/s. The types of material used on ANSYS software were solid 164, orthotropic material for composite, and solid 168 rigid for bullet projectile.

Modeling of loading conditions in this research includes initial velocity, displacement, and contact. In this study, various speeds were used. This displacement loading condition was applied to resist movement, both translational and rotational, on the outer edges of the composite by holding the nodes at each outer corner of the composite, as depicted in Fig. 3.

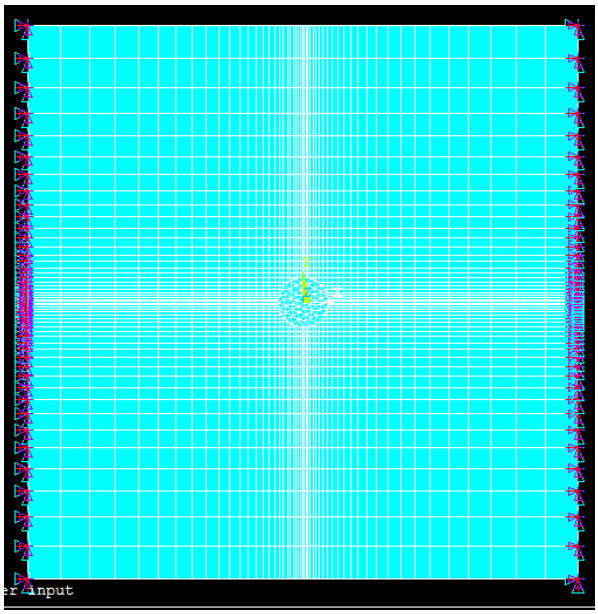

Fig. 3. Displacement loading.

3 Results and Discussion

The directions of composite fibers used in this modeling were [±45°] and [0°,90°]. Therefore, the constant and strength of the composite may change according to the variations in the direction of the composite fibers (Table 3 and Table 4).

Table 3. Composite constants according to fiber direction variations

	Composite constants			
	0^0	90^0	45^0	-45^0
E_1 (GPa)	0.720	0.070	0.497	0.293
E_2 (GPa)	0.070	0.720	0.293	0.497
E_3 (GPa)	0.070	0.070	0.070	0.070
v_{12}	0.351	0.122	0.379	0.093
v_{23}	0.122	0.351	0.093	0.379
v_{13}	0.122	0.122	0.122	0.122

Table 4. Composite strength according to fiber orientation variation

	Strength (GPa)			
	0^0	90^0	45^0	-45^0
X_T	0.720	0.070	0.497	0.293
Y_T	0.070	0.720	0.293	0.497
Z_T	0.070	0.070	0.070	0.070
X_C	0.351	0.122	0.379	0.093
Y_C	0.122	0.351	0.093	0.379
Z_C	0.122	0.122	0.122	0.122
S_{12}	0.102	0.102	0.325	0.325
S_{23}	0.051	0.102	0.036	0.108
S_{13}	0.102	0.051	0.108	0.036

The calculation of the supporting data, the modeling results were obtained in the form of a decline in projectile speed when hitting the composite [±45°] and [0°,90°] in Fig. 4.

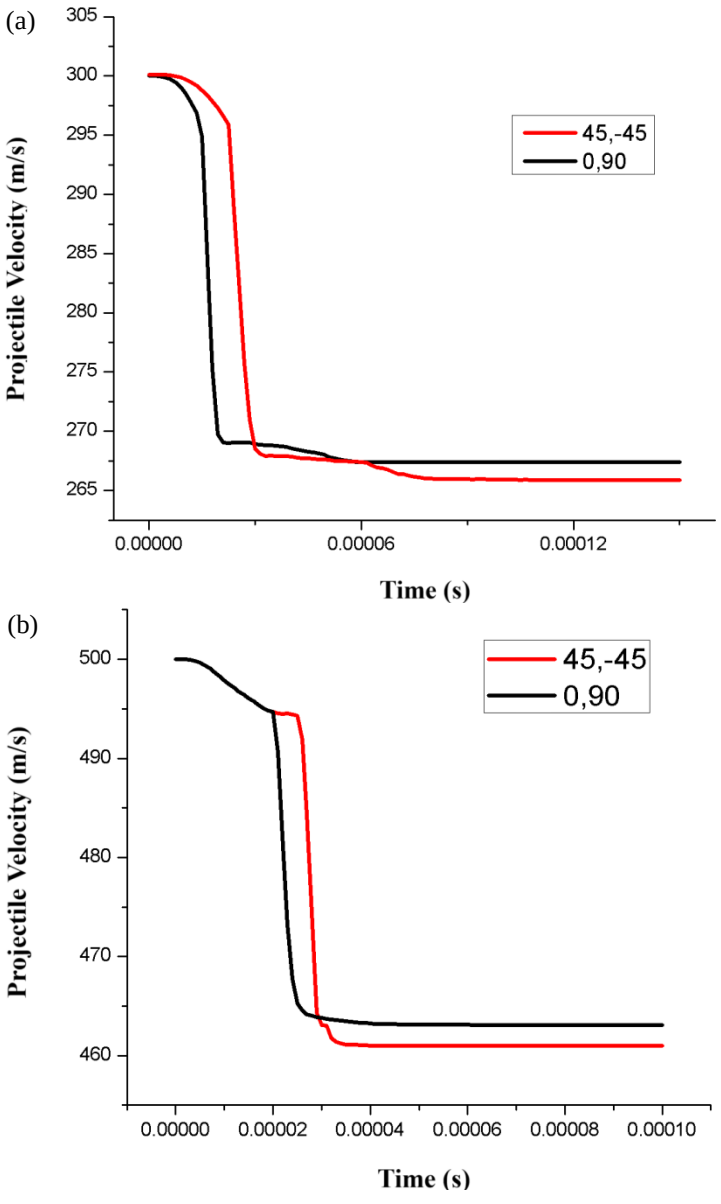

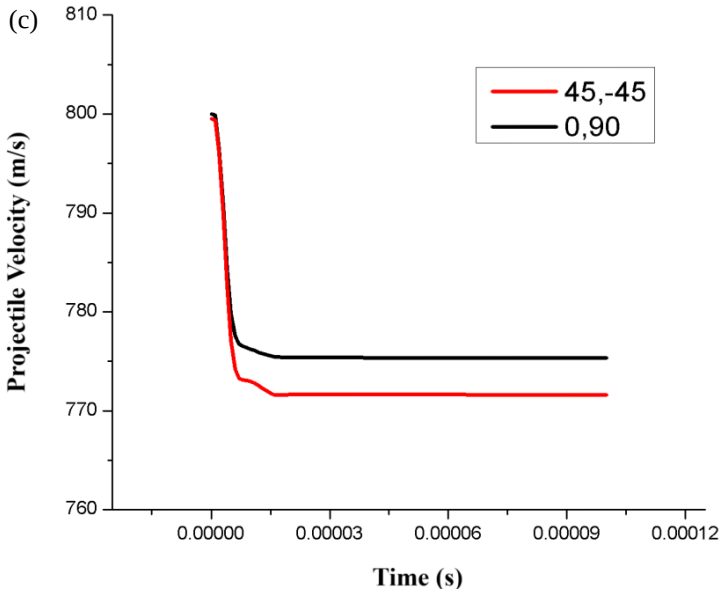

Fig. 4. Composite projectile velocity graphs in [±45°] and [0°,90°] directions: (a) 12 layers at 300 m/s, (b) 12 layers at 500 m/s and (c) 12 layers at 800 m/s.

From Fig. 4, the post-perforation velocity (V_b) and the ballistic limit velocity from the modeling results (V_p) are obtained in Table 5.

Table 5. Ballistic speed limit of the composite in [±45°] and [0°,90°] directions using 12 layers at 300, 500 and 800 m/s

Fiber orientation	V_0 (m/s)	V_p (m/s)	V_b (m/s)
[±45°]	300	265.76	34.24
	500	461.02	38.98
	800	772.07	27.92
[0°,90°]	300	267.40	32.60
	500	463.07	36.93
	800	775.33	24.67

Table 5 shows that the ballistic limit of the modeled results is close to the results of the modeling in the study. The composite with a [±45°] fiber orientation has a ballistic limit that was 16.23% greater than that of the composite with another orientation [0°,90°]. This is because the perforation time of the projectile in the [±45°] fiber-oriented composite was 15.35% longer than in the [0°,90°] fiber-oriented composite, as shown in Fig. 5.

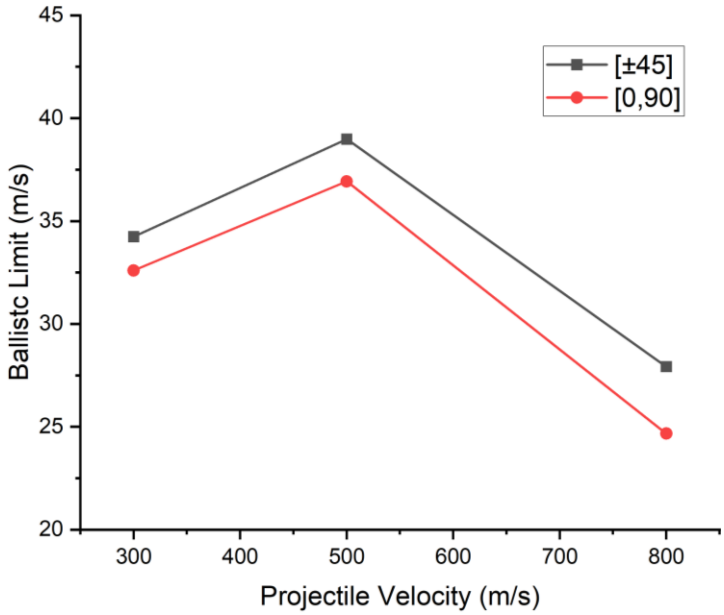

Fig. 5. Ballistic limit of 12 layers composite, [±45°] and [0°,90°] fiber directions vs. 300, 500, 800 m/s projectile speeds.

The duration of perforation time was obtained by taking the difference between the projectile's initial speed just before hitting the composite and the speed after perforating is illustrated in Fig. 6, while the total perforation time is summarized in Table 6.

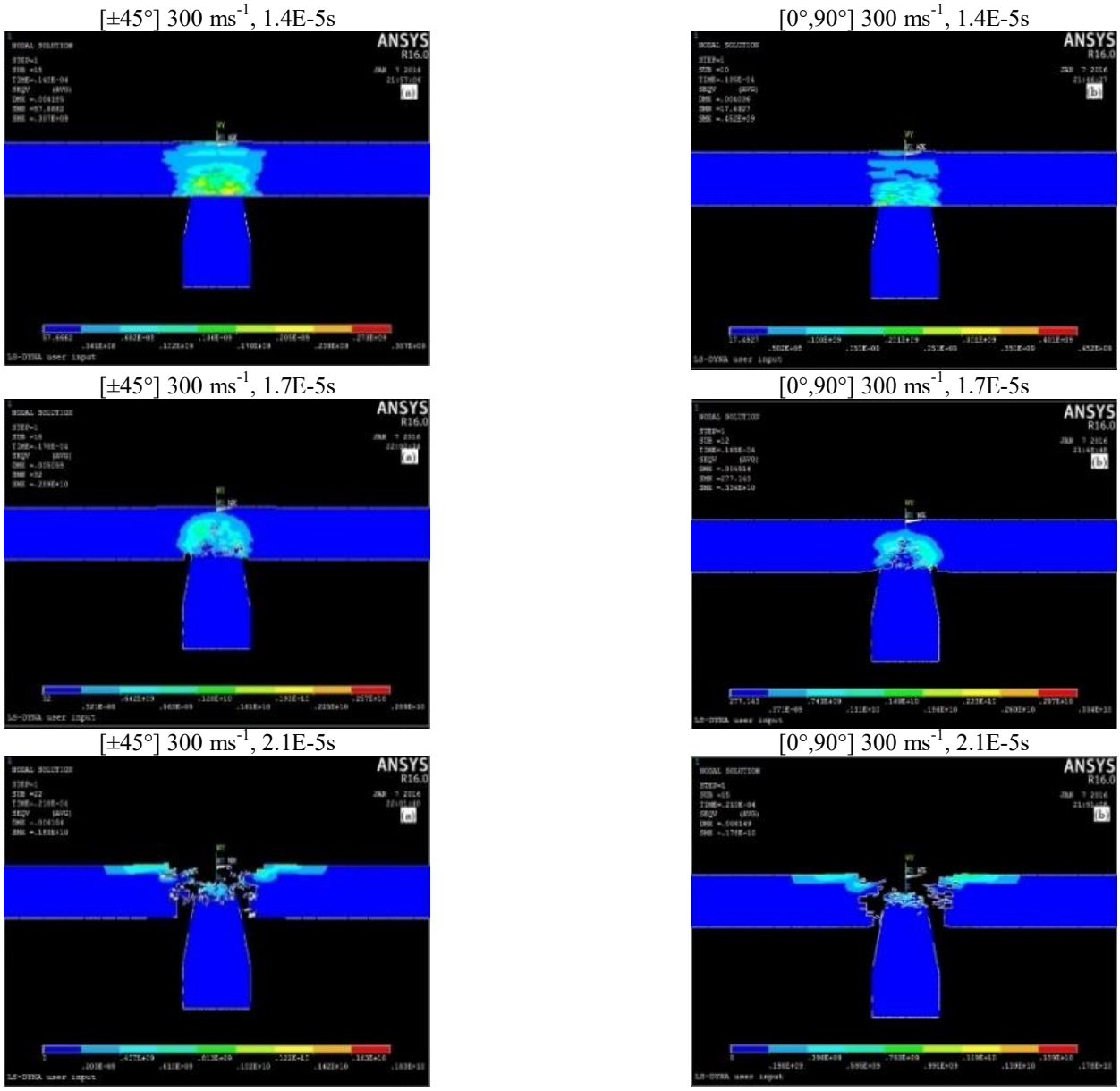

Fig. 6. Von Mises stress distribution with a bullet projectile speed of 300 m/s.

Table 6. Total perforation time for a 12-layer composite at [±45°] and [0°,90°] fiber directions

Fiber orientation	t_0 (s)	t_p (s)	t_{tot} (s)
[±45°]	300	265.76	34.24
	500	461.02	38.98
	800	772.07	27.93
[0°,90°]	300	267.40	32.60
	500	463.07	36.93
	800	775.33	24.67

At each speed of 300, 500, and 800 m/s, the von Mises amount received by the composite was measured three times: at the start, middle, and end of the perforation.

At 1.4E-5s (see Fig. 6), the composite with fiber orientation [±45°] achieved the maximum von Mises stress of 0.307 GPa. In contrast, the composite with a fiber orientation of [0°,90°] had already experienced a von Mises stress of 0.452 GPa. This causes the composite with a [0°,90°] fiber orientation to deteriorate more quickly. In contrast, at 1.7E-5s (Fig. 6), the maximum von Mises stress on the composite with [±45°] fiber orientation was lower, at 2.89 GPa, compared to the [0°,90°] composite, which was at 3.94 GPa as shown in Fig. 6. This is because the composite with [±45°] fiber orientation undergoes perforation more slowly than the [0°,90°] composite. At 2.1E-5s, the maximum von Mises stress on the composite with [±45°] fiber orientation was higher at 1.83 GPa, compared to the [0°,90°] composite, which was at 1.78 GPa. This occurs because the composite with orientation [±45°] is still experiencing perforation, while the composite with [0°,90°] fiber orientation is almost done with perforation (see Fig. 6).

At 2.1E-5s (see Fig. 7), the composite with [±45°] fiber orientation achieved the maximum von Mises stress of 0.208 GPa. In contrast, the [0°,90°] fiber orientation had already experienced a von Mises stress of 0.320 GPa. This causes the composite with [0°,90°] fiber orientation to deteriorate more quickly. In contrast, at 1.2E-5s (Fig. 7), the maximum von Mises stress on the composite with [±45°] fiber orientation was lower, at 2.49 GPa, compared to the [0°,90°] composite, which was at 2.92 GPa as shown in Fig. 7. This is because the [±45°] fiber orientation undergoes perforation more slowly than the [0°,90°] composite. As shown in the figure, the composite with [0°,90°] fiber orientation had experienced damage much earlier. At 2.2E-4s, the maximum von Mises stress on the composite with [±45°] fiber orientation was higher at 1.34 GPa, compared to the [0°,90°] composite, which was at 1.33 GPa. This occurs because the composite with orientation [±45°] has just started to experience damage, while the composite with [0°,90°] fiber orientation has fully deteriorated (see Fig. 7).

[±45°] 500 ms^{-1}, 2.1E-5s

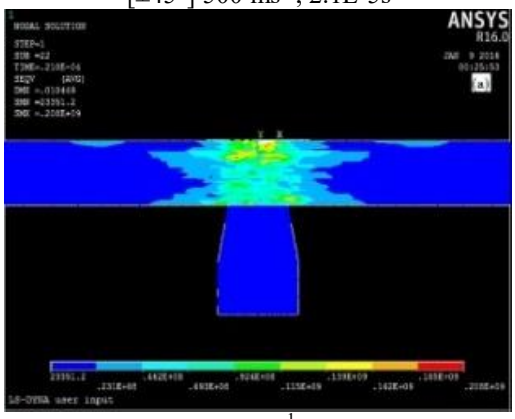

[0°,90°] 500 ms^{-1}, 2.1E-5s

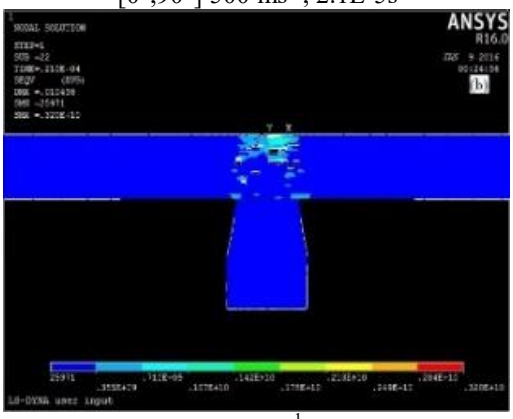

[±45°] 500 ms^{-1}, 2.2E-5s

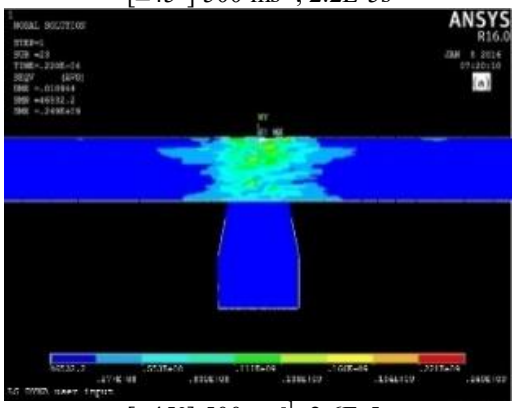

[0°,90°] 500 ms^{-1}, 2.2E-5s

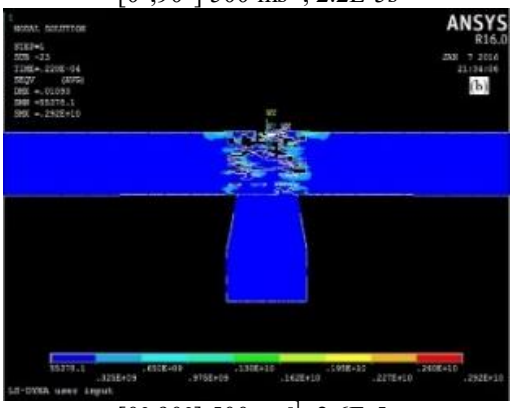

[±45°] 500 ms^{-1}, 2.6E-5s

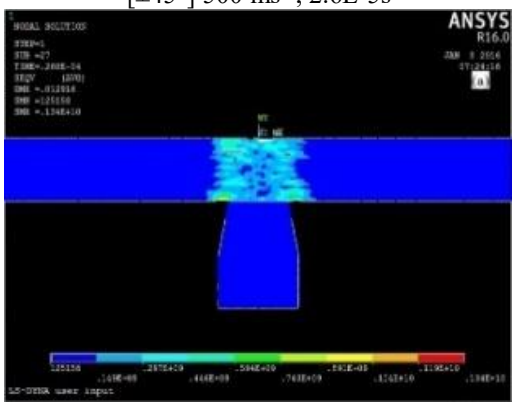

[0°,90°] 500 ms^{-1}, 2.6E-5s

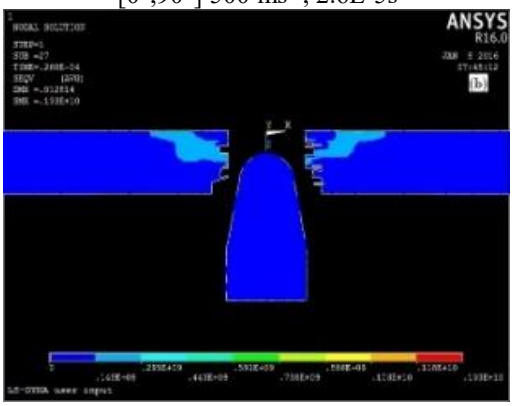

Fig. 7. Von Mises stress distribution with a bullet projectile speed of 500 m/s.

At 0.3E-5s (see Fig. 8), the composite with [±45°] fiber orientation achieved the maximum von Mises stress of 8.22 GPa. In contrast, the [0°,90°] fiber orientation had already reached a von Mises stress of 9.13 GPa. This causes the composite with [0°,90°] fiber orientation to deteriorate more quickly. In contrast, at 0.5E-5s (see Fig. 8), the maximum von Mises stress on the composite with [±45°] fiber orientation was lower, at 6.73 GPa, compared to the [0°,90°] composite, which was at 7.05 GPa. This is because [±45°] fiber orientation undergoes perforation more slowly than the [0°,90°] composite. The figure shows that [0°,90°] fiber orientation of composite had already suffered more severe damages. At 0.8e-4s, a similar pattern was observed: the maximum von Mises stress on the composite with [±45°] fiber orientation was higher, at 4.04 GPa, compared to the [0°,90°] composite, which was at 1.56 GPa. This occurs because the composite with [±45°] fiber orientation was still undergoing perforation, while the composite with orientation [0°,90°] was almost done with perforation (see Fig. 8).

[±45°] 800 ms^{-1}, 0.3E-5s

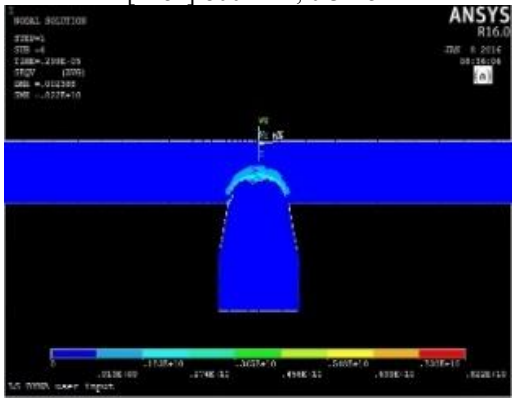

[0°,90°] 800 ms^{-1}, 0.3E-5s

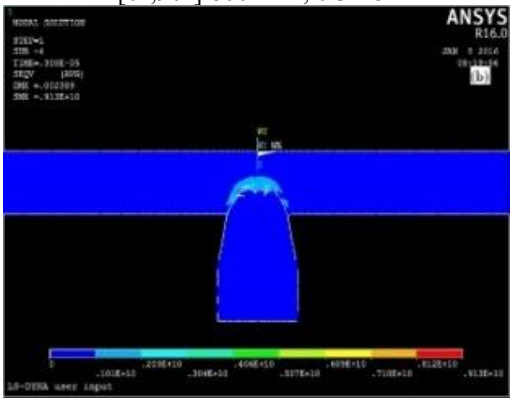

[±45°] 800 ms^{-1}, 0.5E-5s

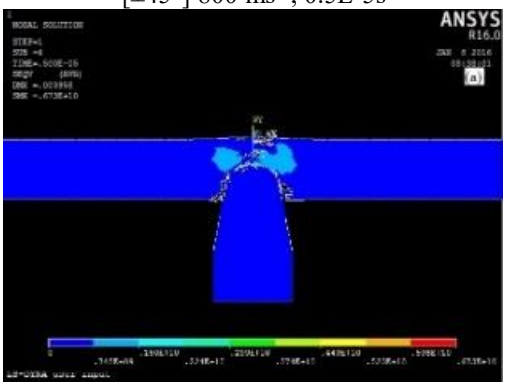

[0°,90°] 800 ms^{-1}, 0.5E-5s

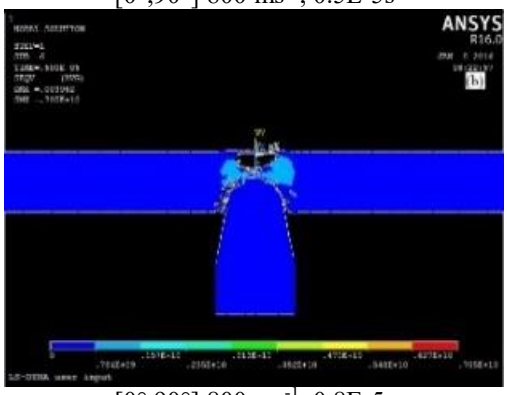

[±45°] 800 ms^{-1}, 0.8E-5s

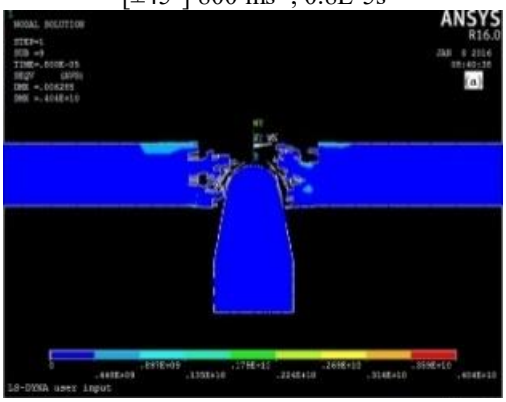

[0°,90°] 800 ms^{-1}, 0.8E-5s

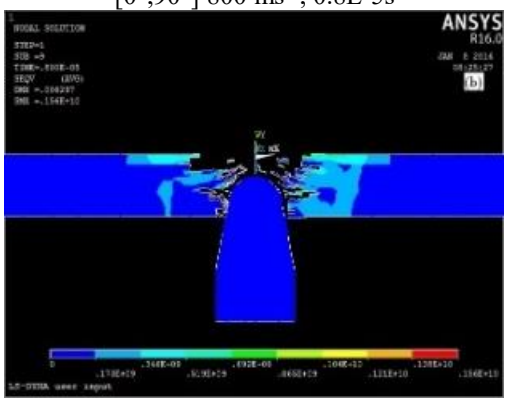

Fig. 8. The distribution of von Mises stress with a bullet projectile speed of 800 m/s.

Changing the direction of E-glass composite reinforcing fibers/isophthalic polyester from [0°,90°] to [±45°] also affects the ballistic impact strength. Using the ballistic speed limit data in Table 5, the ballistic strength of the composite fiber direction [±45°] and [0°,90°] is obtained in Table 7.

Table 7. Ballistic strength of the composite [±45°] and [0°,90°]

Fiber orientation	$\mathbf{V_0}$ (m/s)	Ballistic strength (MPa)
[±45°]	300	9.35
	500	12.10
	800	6.20
[0°,90°]	300	8.47
	500	10.87
	800	4.85

From Table 7, it can be concluded that the ballistic strength of the composite with [±45°] orientation was 16.51% higher than the composite with the fiber direction [0°,90°]. To better illustrate the difference in ballistic strength between these fiber directions, a graph is provided in Fig. 9.

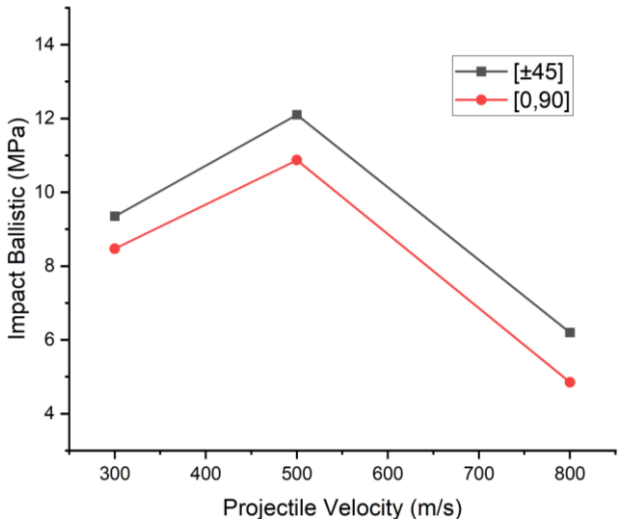

Fig. 9. The comparison of ballistic strength of composites [±45°] and [0°,90°].

To validate the obtained results, the Wen's ballistic model [7] was employed. In Table 8, the composite ballistic speed limits [±45°] and [0°,90°] calculated by the Wen's model are presented.

Table 8. Ballistic limit of the Wen's model

Fiber orientation	Layer number	$\boldsymbol{V_b}$ (m/s)
[±45°]	12	33.69
[0°,90°]	12	29.43

The relative error value was determined from the percentage difference between the ballistic speed limit calculated by the Wen's model (V_b) and the modeling results (V_M). Table 9 shows that the highest relative error that occurred was 20.64%. The results indicated that the finite element model demonstrates in predicting the effect of fiber orientation on the ballistic impact strength of E-glass/isophthalic polyester composites.

Table 9. Relative error in composites with 12 layers

Fiber orientation	Projectile speed (m/s)	V_M (m/s)	$\boldsymbol{V_b}$ (m/s)	Relative error (%)
[±45°]	300	33.69	34.24	1.62
	500	33.69	38.98	13.58
	800	33.69	27.93	-20.64
[0°,90°]	300	29.43	32.60	9.71
	500	29.43	36.93	20.30
	800	29.43	24.67	-19.32

4 Conclusion

Based on this research, several key findings are highlighted. The 12-layer E-glass/isophthalic polyester composite with a fiber orientation of [±45°] had 16.51% higher ballistic strength than with fiber orientations of [0°, 90°]. The highest ballistic impact strength for the [±45] fiber orientation occurred at a velocity of 500 m/s, outperforming the 300 m/s and 800 m/s velocities by 12.92% and 43.81%, respectively. Validation using the Wen model confirmed the accuracy of the simulation, with relative error values ranging between 1.62% and 20.64%.

References

[1] A. S. Kshatriya, A. S. Kshatriya, A. Kumar Mishra, and V. S. Janani kavi Priya, "Jute and E-glass fiber-reinforced polypropylene composites: Comparative study," *Mater. Today Proc.*, Sep. 2023, doi: 10.1016/j.matpr.2023.08.231.

[2] H. M. Naguib and G. Hou, "Vinylester-glass fiber composite for water pipe: Processing and effect of fiber direction," *Egypt. J. Pet.*, vol. 32, no. 3, pp. 24–30, Sep. 2023, doi: 10.1016/j.ejpe.2023.08.001.

[3] H. M. Naguib and X. H. Zhang, "Advanced recycled polyester based on PET and oleic acid," *Polym. Test.*, vol. 69, pp. 450–455, Aug. 2018, doi: 10.1016/j.polymertesting.2018.05.049.

[4] J. Xu *et al.*, "Hybridization effects on ballistic impact behavior of carbon/ aramid fiber reinforced hybrid composite," *Int. J. Impact Eng.*, vol. 181, p. 104750, Nov. 2023, doi: 10.1016/j.ijimpeng.2023.104750.

[5] R. Hsissou, R. Seghiri, Z. Benzekri, M. Hilali, M. Rafik, and A. Elharfi, "Polymer composite materials: A comprehensive review," *Compos. Struct.*, vol. 262, p. 113640, Apr. 2021, doi: 10.1016/j.compstruct.2021.113640.

[6] D. P. Armstrong, K. Chatterjee, T. K. Ghosh, and R. J. Spontak, "Form-stable phase-change elastomer gels derived from thermoplastic elastomer copolyesters swollen with fatty acids," *Thermochim. Acta*, vol. 686, p. 178566, Apr. 2020, doi: 10.1016/j.tca.2020.178566.

[7] K. Senthilkumar *et al.*, "Evaluation of mechanical and free vibration properties of the pineapple leaf fibre reinforced polyester composites," *Constr. Build. Mater.*, vol. 195, pp. 423–431, Jan. 2019, doi: 10.1016/j.conbuildmat.2018.11.081.

[8] S. Zhu *et al.*, "Enhanced interfacial interactions by PEEK-grafting and coupling of acylated CNT for GF/PEEK composites," *Compos. Commun.*, vol. 18, pp. 43–48, Apr. 2020, doi: 10.1016/j.coco.2020.01.008.

[9] K. K. Chawla, *Composite Materials: Science and Engineering*. Springer Science & Business Media, 2012.

[10] S. Alam and P. Aboagye, "Numerical Modeling on Ballistic Impact Analysis of the Segmented Sandwich Composite Armor System," *Appl. Mech.*, vol. 5, no. 2, Art. no. 2, Jun. 2024, doi: 10.3390/applmech5020020.

[11] D. Ma, R. Scazzosi, and A. Manes, "Modeling approaches for ballistic simulations of composite materials: Analytical model vs. finite element method," *Compos. Sci. Technol.*, vol. 248, p. 110461, Mar. 2024, doi: 10.1016/j.compscitech.2024.110461.

[12] C. Cong, W. Zhu, J. Liu, and X. Wei, "A review on the analytical and numerical models for ballistic limit of fiber-reinforced composites," *Compos. Struct.*, vol. 345, p. 118392, Oct. 2024, doi: 10.1016/j.compstruct.2024.118392.

[13] B. Elamvazhudi and D. Boodala, "Ballistic impact study on fibre reinforced polymer composites using FEA," *Mater. Today Proc.*, Feb. 2023, doi: 10.1016/j.matpr.2023.02.135.

[14] V. Mahesh, S. Joladarashi, and S. M. Kulkarni, "Influence of thickness and projectile shape on penetration resistance of the compliant composite," *Def. Technol.*, vol. 17, no. 1, pp. 245–256, Feb. 2021, doi: 10.1016/j.dt.2020.03.006.

[15] M. I. Ammarullah *et al.*, "Minimizing Risk of Failure from Ceramic-on-Ceramic Total Hip Prosthesis by Selecting Ceramic Materials Based on Tresca Stress," *Sustainability*, vol. 14, no. 20, Art. no. 20, Jan. 2022, doi: 10.3390/su142013413.

[16] L. H. Nguyen, T. R. Lässig, S. Ryan, W. Riedel, A. P. Mouritz, and A. C. Orifici, "A methodology for hydrocode analysis of ultra-high molecular weight polyethylene composite under ballistic impact," *Compos. Part Appl. Sci. Manuf.*, vol. 84, pp. 224–235, May 2016, doi: 10.1016/j.compositesa.2016.01.014.

[17] P. Karthick and K. Ramajeyathilagam, "Numerical study on ballistic impact behavior of hybrid composites," *Mater. Today Proc.*, vol. 59, pp. 995–1003, Jan. 2022, doi: 10.1016/j.matpr.2022.02.270.

[18] H. M. Wen, "Predicting the penetration and perforation of FRP laminates struck normally by projectiles with different nose shapes," *Compos. Struct.*, vol. 49, no. 3, pp. 321–329, Jul. 2000, doi: 10.1016/S0263-8223(00)00064-7.

[19] "Ballistic Resistance of Personal Body Armor, NIJ Standard-0101.04 | National Institute of Justice." Accessed: Sep. 27, 2024. [Online]. Available: https://nij.ojp.gov/library/publications/ballistic-resistance-personal-body-armor-nij-standard-010104

[20] D. B. Miracle, Ed., *ASM handbook. 21: Composites / Daniel B. Miracle ... Volume chairs*, 5. print. Materials Park, Ohio: ASM International, 2007.

[21] P. Zochowski *et al.*, "Comparison of Numerical Simulation Techniques of Ballistic Ceramics under Projectile Impact Conditions," *Materials*, vol. 15, no. 1, Art. no. 1, Jan. 2022, doi: 10.3390/ma15010018.

[22] A. Wiśniewski and M. Gmitrzuk, "Validation of numerical model of the Twaron CT709 ballistic fabric," *Proc. - 27th Int. Symp. Ballist. Ballist. 2013*, vol. 2, pp. 1535–1544, Jan. 2013.